SUPPORTING INFORMATION

Insights into mapping tropical primary wet forests in the Amazon Basin from satellite-based time series metrics of canopy stability

Brendan Mackey[1], Sonia Hugh[1], Tatiana Shestakova[2,3], Brendan Rogers[2] and Ludmila Rattis[2]

[1]Griffith University, Engineering Drive, Southport 2022, Queensland Australia
[2]Woodwell Climate Research Center, Falmouth, MA, United States
[3]Department of Agricultural and Forest Sciences and Engineering University of Lleida, Lleida, Spain

SI.1 Supporting figures and tables

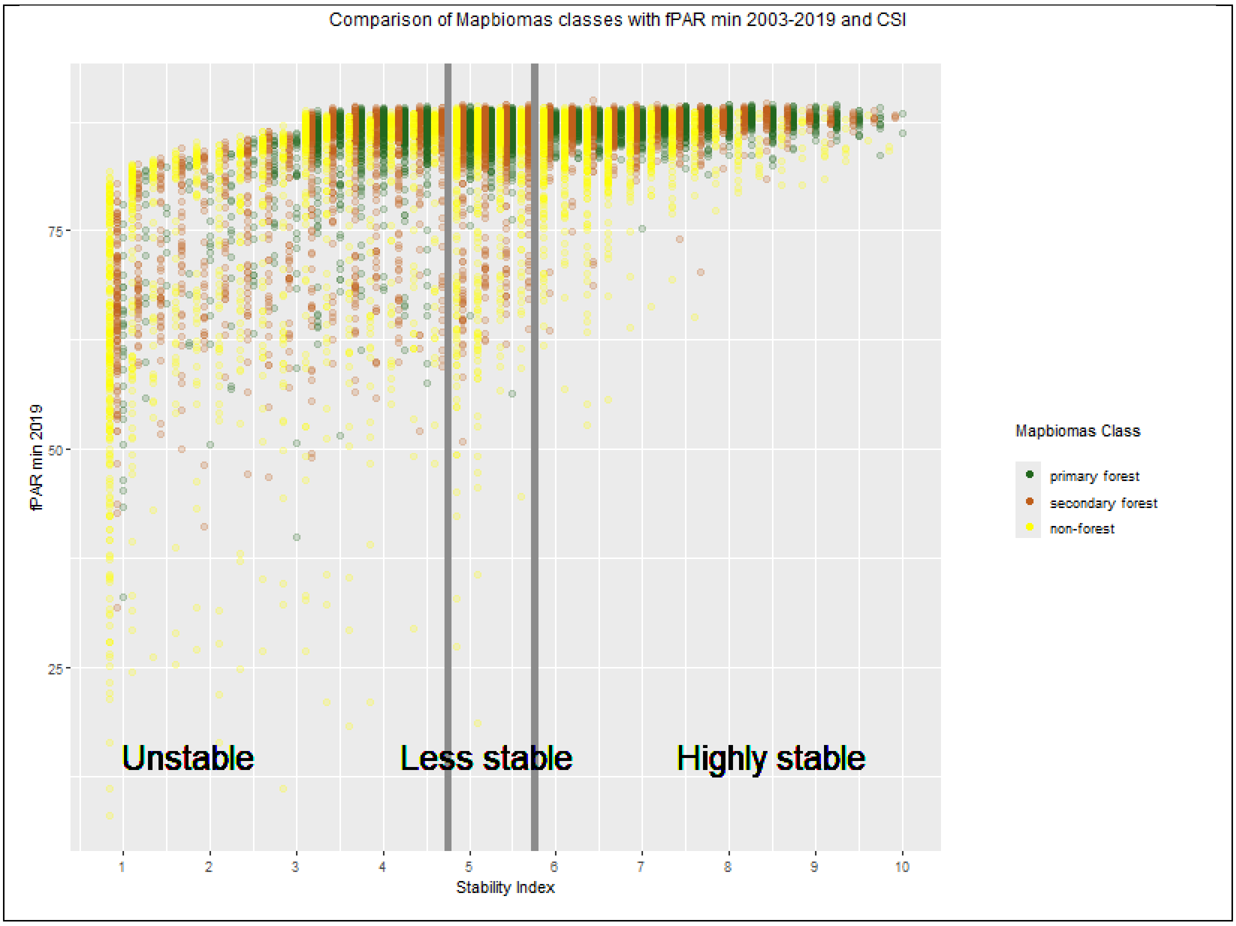

Figure SI1. Density scatter plot of the three MapBiomass forest classes (primary forest, secondary forest, non-forest) in relation to fPAR_min in 2019 and the Canopy Stability Index (CSI) classes (4-40). We used the CSI class value of 20 to distinguish our “highly stable” from “more unstable” category as this delineated 75% of MapBiomas primary forest. CSI class value 25 was used to distinguish our “more unstable” from “unstable” category as this delineated where 75% of the MapBiomas secondary forest and non-forest areas occurred. The index values were then simplified to classes 1-10 and reversed with unstable (1) to stable (10).

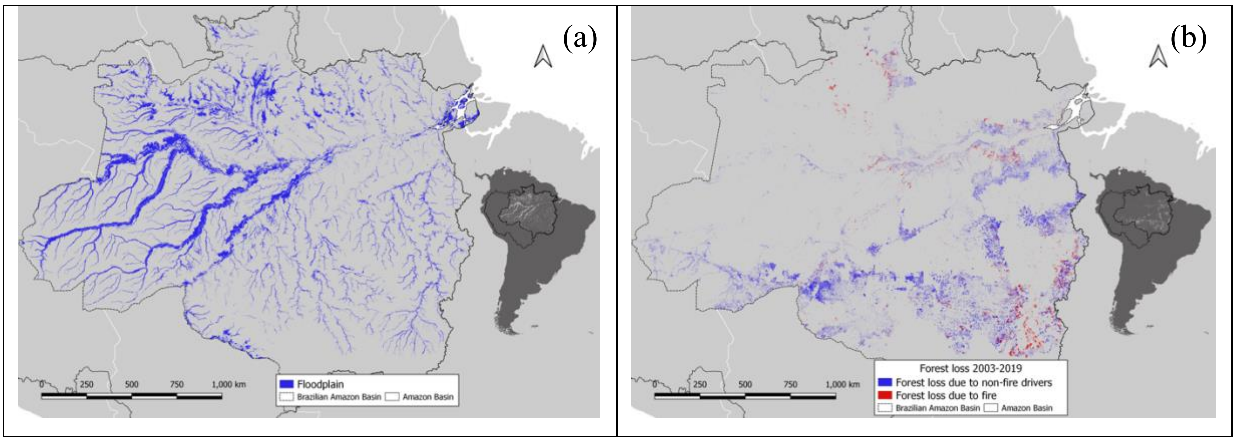

Figure SI2. Spatial data used for flood plains (a) and burned forest for the Brazilian Amazon (b). Sources: (Nardi et al., 2019; Tyukavina et al., 2022) respectively.

Figure SI3. Percent error for downscaled Mapbiomas pixels.

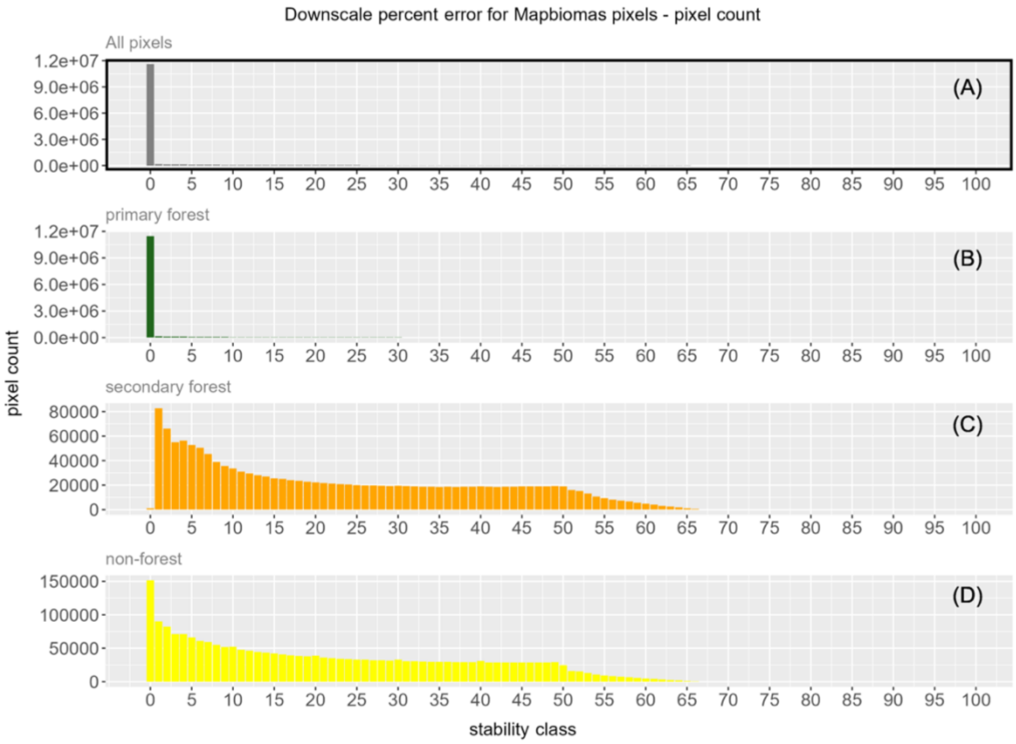

Figure SI3. Downscale percent error for Mapbiomas pixels. Shows the distribution of percent error of Mapbiomas pixels (30m) when upscaled to MODIS resolution (~500m). The error distribution for (A) all pixels and the Mapbiomas classes of (B) primary forest, (C) secondary forest and (D) non-forest pixels.

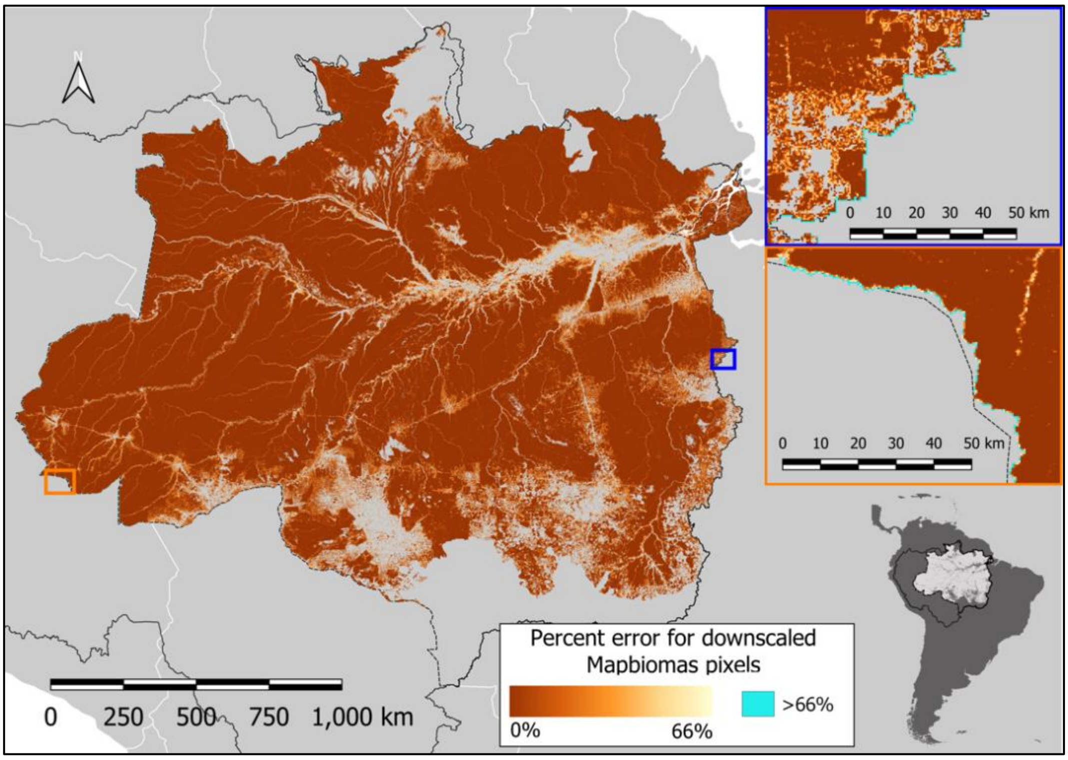

Figure SI4. Spatial distribution of percent error for downscaled Mapbiomas pixels.

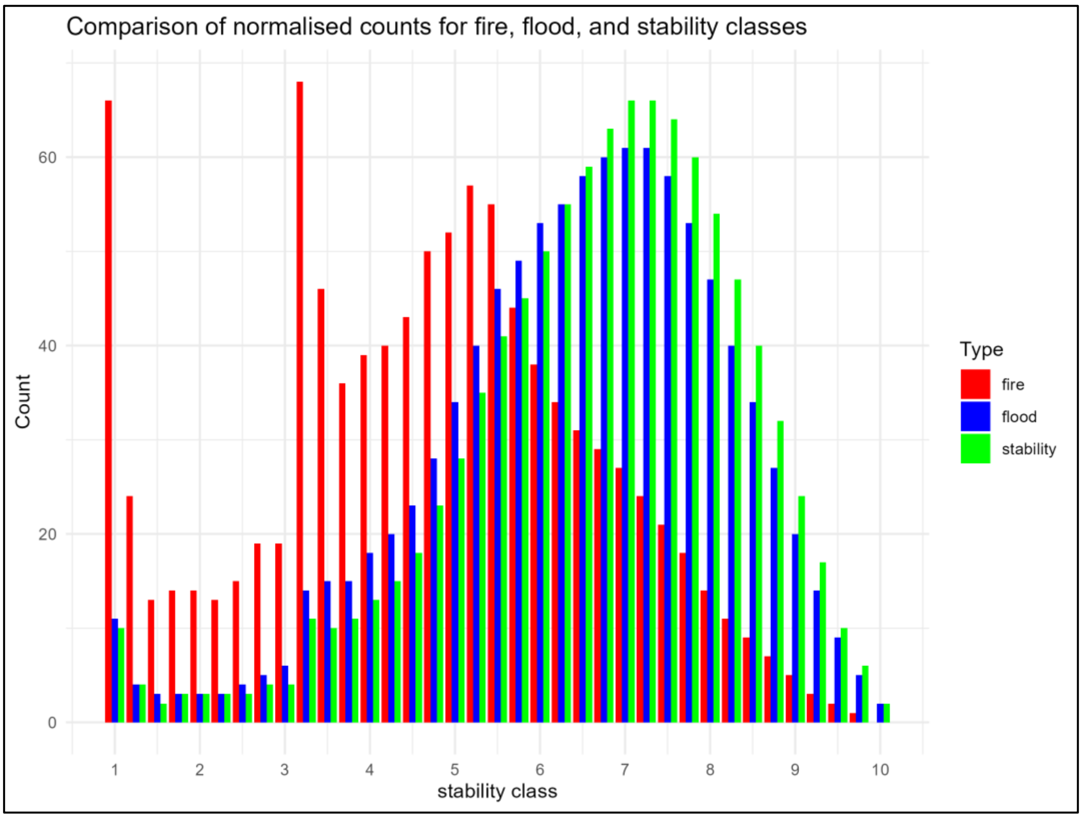

Figure SI5. Normalised counts for forest CSI for pixels that experienced fires during the period 2003-2019, occur on seasonally flooded landscapes and all pixels within the study area. There are multiple bars for each stability class because they represent the original range of values which ranged from 4-40. In order to derive the 10-class stability index plotted on the x-axis, the 4-40 classes were divided by 4.

Table SI1. Details statistics of the comparison between the three forest stability index classes (highly stable, less stable, unstable) and the three MapBiomas classes (primary forest, secondary forest, non-forest)

Ecoregion	Highly stable/primar forest	Less stable/primar forest	Unstable/prim forest	Highly stable/second forest	Less stable/second forest	Unstable/secc forest	Stable/non-forest	Less stable/non-forest	Unstable/non forest
Guianan Highlands moist forests	50743 (46.5%)	30 (0.0%)	39 (0.0%)	23525 (21.6%)	26 (0.0%)	86 (0.1%)	34131 (31.3%)	61 (0.1%)	486 (0.4%)
Guianan piedmont moist forests	280964 (72.4%)	102 (0.0%)	122 (0.0%)	54955 (14.2%)	90 (0.0%)	284 (0.1%)	49142 (12.7%)	260 (0.1%)	2297 (0.6%)
Japurá-Solimões	835143 (81.0%)	657 (0.1%)	1910 (0.2%)	122782 (11.9%)	410 (0.0%)	1885 (0.2%)	60321 (5.9%)	641 (0.1%)	7278 (0.7%)
Marajó várzea	55175 (61.8%)	292 (0.3%)	379 (0.4%)	18233 (20.4%)	505 (0.6%)	367 (0.4%)	12237 (13.7%)	976 (1.1%)	1186 (1.3%)
Pantepui forests & shrublands	1316 (17.9%)	0 (0.0%)	4 (0.1%)	1389 (18.8%)	1 (0.0%)	2 (0.0%)	4529 (61.5%)	13 (0.2%)	115 (1.6%)
Purus-Madeira moist forests	619914 (80.7%)	1050 (0.1%)	1775 (0.2%)	76958 (10.0%)	746 (0.1%)	4698 (0.6%)	37536 (4.9%)	1739 (0.2%)	23627 (3.1%)
Rio Negro campinarana	192334 (63.0%)	6 (0.0%)	500 (0.2%)	57542 (18.8%)	14 (0.0%)	587 (0.2%)	51647 (16.9%)	50 (0.0%)	2812 (0.9%)
Tapajós-Xingu moist forests	1051382 (72.0%)	2975 (0.2%)	5408 (0.4%)	163561 (11.2%)	2442 (0.2%)	13389 (0.9%)	126167 (8.6%)	5230 (0.4%)	90066 (6.2%)
Caqueta moist forests	41794 (70.0%)	0 (0.0%)	28 (0.0%)	11829 (19.8%)	0 (0.0%)	25 (0.0%)	6037 (10.1%)	0 (0.0%)	24 (0.0%)
Guianan lowland moist forests	108079 (70.9%)	4 (0.0%)	3 (0.0%)	31882 (20.9%)	1 (0.0%)	2 (0.0%)	12499 (8.2%)	2 (0.0%)	2 (0.0%)
Gurupa várzea	3387 (20.7%)	234 (1.4%)	225 (1.4%)	2938 (18.0%)	332 (2.0%)	387 (2.4%)	4874 (29.8%)	1103 (6.7%)	2866 (17.5%)
Juruá-Purus moist forests	961623 (85.4%)	487 (0.0%)	554 (0.0%)	130361 (11.6%)	289 (0.0%)	750 (0.1%)	28896 (2.6%)	379 (0.0%)	2087 (0.2%)
Madeira-Tapajós moist forests	1802918 (72.4%)	7169 (0.3%)	9893 (0.4%)	247543 (9.9%)	4767 (0.2%)	25026 (1.0%)	174953 (7.0%)	10860 (0.4%)	205670 (8.3%)
Mato Grosso tropical dry forests	588024 (54.8%)	1649 (0.2%)	2299 (0.2%)	132013 (12.3%)	1794 (0.2%)	6301 (0.6%)	204031 (19.0%)	10429 (1.0%)	126752 (11.8%)
Monte Alegre várzea	148857 (67.4%)	2441 (1.1%)	2056 (0.9%)	28441 (12.9%)	1557 (0.7%)	2625 (1.2%)	21638 (9.8%)	2707 (1.2%)	10530 (4.8%)
Negro-Branco moist forests	169187 (79.2%)	37 (0.0%)	191 (0.1%)	26598 (12.4%)	49 (0.0%)	188 (0.1%)	16606 (7.8%)	58 (0.0%)	749 (0.4%)
Purus várzea	441281 (71.5%)	1507 (0.2%)	2333 (0.4%)	100335 (16.3%)	891 (0.1%)	3030 (0.5%)	55306 (9.0%)	1415 (0.2%)	11112 (1.8%)
Solimões-Japurá moist forests	133026 (79.0%)	28 (0.0%)	53 (0.0%)	25984 (15.4%)	8 (0.0%)	42 (0.0%)	9059 (5.4%)	15 (0.0%)	109 (0.1%)
Southwest Amazon moist forests	932936 (64.6%)	542 (0.0%)	4352 (0.3%)	321349 (22.2%)	512 (0.0%)	10608 (0.7%)	151546 (10.5%)	1102 (0.1%)	21841 (1.5%)
Uatumã-Trombetas moist forests	1489842 (78.0%)	4980 (0.3%)	4671 (0.2%)	225629 (11.8%)	2846 (0.1%)	7122 (0.4%)	139100 (7.3%)	5619 (0.3%)	29032 (1.5%)
Xingu-Tocantins-Araguaia moist forests	287746 (63.1%)	313 (0.1%)	1602 (0.4%)	51391 (11.3%)	342 (0.1%)	6102 (1.3%)	53412 (11.7%)	1139 (0.2%)	53973 (11.8%)
Iquitos várzea	57012 (47.4%)	209 (0.2%)	1525 (1.3%)	28372 (23.6%)	168 (0.1%)	3075 (2.6%)	21522 (17.9%)	354 (0.3%)	8134 (6.8%)

SI.2 Methods for Canopy Stability Index (CSI) Calculation

We calculated the Canopy Stability Index (CSI) using a modified version of the stability index from Shestakova et al. (2022). Our calculation incorporated four canopy metrics derived from a 2003-2019 time series: (1) the Coefficient of Variation (CoV) of annual mean fPAR, (2) the absolute slope of the fPAR time series, (3) the CoV of annual mean SIWSI, and (4) the absolute slope of the SIWSI time series.

Model Inputs

This study utilized a 17-year monthly time series (2003–2019) of fPAR (fraction of photosynthetically active radiation intercepted by the canopy) and SIWSI (shortwave infrared water stress index), both sourced from MODIS satellite imagery at ~500 m (463 m) resolution. The fPAR index, representing absorbed solar radiation in the 400–700 nm range, was derived from the MCD15A3H v6 Leaf Area Index/FPAR 4-day global product [1]. SIWSI was calculated using the near-infrared (NIR; 841–876 nm) and shortwave infrared (SWIR; 1628–1652 nm) bands of the MOD09A1 v6 Terra Surface Reflectance 8-Day Global product [2] as follows:

$$SIWSI = (SWIR+NIR)/(SWIR-NIR)$$

Quality flags were used to exclude pixels impacted by cloud contamination and sensor errors, removing pixels with high aerosol levels, cirrus, clouds, or cloud shadows.

Input Constraints and Masks

The analysis was constrained to the years 2003–2019, aligning with the most recent MapBIOMAS deforestation map available at the time (2022). All months were included in calculations. Following prior research, which demonstrated that fPAR/SIWSI indices must be analyzed within comparable forest ecosystem types for accurate stability assessment [3,4], we masked the 2003 forest cover to exclude tropical montane areas [5], limiting the study area to tropical and subtropical moist broadleaf forests [6].

To capture the impact of seasonal dry periods on forest phenology, the study used the Standardised Precipitation Evapotranspiration Index (SPEI) calculated with the SPEI package [7,8] in R [9], based on Thorntwaite's potential evapotranspiration model. SPEI provides a multiscalar measure that accounts for temperature variability, crucial for drought assessment [7], using temperature data from the ERA5 Monthly Aggregates [10] and precipitation data from the Global Precipitation Measurement (GPM) dataset [11]. SPEI was computed for the 2003–2019 period, with monthly means calculated for each pixel to identify the driest month for each pixel.

Based on monthly minimum SPEI values, pixels were grouped into three hydro-climatic regions representing seasonal variations in Brazil: region 1 (blue) with dry periods from December–April, region 2 (yellow) from May–July, and region 3 (green) from August–November.

CSI Calculations

The CSI calculation required two key statistics for each of the four metrics: (i) the Coefficient of Variation (CoV) for interannual variability, and (ii) the absolute slope of each time series, representing change over time. We first generated mean monthly time series for both fPAR and SIWSI, then calculated annual means for each pixel (17 values per pixel) and computed the CoV over these annual means. The absolute slope was obtained by performing a linear regression on the time series and taking the absolute value.

After computing the four metrics (CoV of annual mean fPAR, absolute slope of fPAR, CoV of annual mean SIWSI, and absolute slope of SIWSI), each metric was ranked and classified into 10 deciles (bins) from 1–10. These decile values were summed for each pixel, resulting in an initial index range from 4 (most stable) to 40 (least stable). This index was divided by 10 and inverted, yielding a CSI score from 1 (most unstable) to 10 (most stable). CSI calculations were performed separately for each SPEI region, and the results were combined to generate the final index. All calculations were conducted in Google Earth Engine.

References

1. Fensholt, R.; Sandholt, I. Derivation of a Shortwave Infrared Water Stress Index from MODIS Near- and Shortwave Infrared Data in a Semiarid Environment. *Remote Sens. Environ.* **2003**, *87*, 111–121, doi:10.1016/j.rse.2003.07.002.

2. Briant, G.; Gond, V.; Laurance, S.G.W. Habitat Fragmentation and the Desiccation of Forest Canopies: A Case Study from Eastern Amazonia. *Biol. Conserv.* **2010**, *143*, 2763–2769, doi:10.1016/j.biocon.2010.07.024.

3. Shestakova, T.A.; Mackey, B.; Hugh, S.; Dean, J.; Kukavskaya, E.A.; Laflamme, J.; Shvetsov, E.G.; Rogers, B.M. Mapping Forest Stability within Major Biomes Using Canopy Indices Derived from MODIS Time Series. *Remote Sens.* **2022**, *14*, 3813, doi:10.3390/rs14153813.

4. Mackey, B.; Berry, S.; Hugh, S.; Ferrier, S.; Harwood, T.D.; Williams, K.J. Ecosystem Greenspots: Identifying Potential Drought, Fire, and Climate-Change Micro-Refuges. *Ecol. Appl.* **2012**, *22*, 1852–1864, doi:10.1890/11-1479.1.

5. FAO Global Ecological Zones for Fao Forest Reporting: 2010 Update. Forest Resources Assessment Working Paper 179. 2012.

6. Dinerstein, E.; Olson, D.; Joshi, A.; Vynne, C.; Burgess, N.D.; Wikramanayake, E.; Hahn, N.; Palminteri, S.; Hedao, P.; Noss, R.; et al. An Ecoregion-Based Approach to Protecting Half the Terrestrial Realm. *BioScience* **2017**, *67*, 534–545, doi:10.1093/biosci/bix014.

7. Vicente-Serrano, S.M.; Beguería, S.; López-Moreno, J.I. A Multiscalar Drought Index Sensitive to Global Warming: The Standardized Precipitation Evapotranspiration Index. *J. Clim.* **2010**, *23*, 1696–1718, doi:10.1175/2009JCLI2909.1.

8. Beguería, S.; Vicente-Serrano, S.M.; Reig, F.; Latorre, B. Standardized Precipitation Evapotranspiration Index (SPEI) Revisited: Parameter Fitting, Evapotranspiration Models, Tools, Datasets and Drought Monitoring. *Int. J. Climatol.* **2014**, *34*, 3001–3023, doi:10.1002/joc.3887.

9. R Core Team R: A Language and Environment for Statistical Computing 2022.

10. Copernicus Climate Change Service (C3S) ERA5: Fifth Generation of ECMWF Atmospheric Reanalyses of the Global Climate. 2017.

11. Huffman, G.J. *NASA Global Precipitation Measurement (GPM) Integrated Multi-satellitE Retrievals for GPM (IMERG). Algorithm Theoretical Basis Document (ATBD) Version 4.6*; National Aeronautics and Space Administration (NASA), 2017;